Biochemistry

 Volume 36, Number 35 September 2, 1997

Articles

Biochemical and Spectroscopic Characterization of Two New Cytochromes Isolated from *Desulfuromonas acetoxidans*

Mireille Bruschi,*,‡ Mireille Woudstra,‡ Bruno Guigliarelli,‡ Marcel Asso,‡ Elisabeth Lojou,‡ Yves Petillot,§ and Chantal Abergel||

Laboratoire de Bioénergétique et Ingénierie des Protéines, Laboratoire d'Information Génétique et Structurale, IFR 1, C.N.R.S., 31, chemin Joseph Aiguier, 13402 Marseille Cedex 20, France, and Institut de Biologie Structurale, 41 avenue des Martyrs, 38027 Grenoble Cedex 1, France

Received April 3, 1997; Revised Manuscript Received May 28, 1997[⊗]

ABSTRACT: The multimeric cytochromes described to date in sulfate- and sulfur-reducing bacteria are associated with diverse respiratory modes involving the use of elemental sulfur or oxidized sulfur compounds as terminal acceptors. They exhibit no structural similarity with the other cytochrome *c* classes and are characterized by a bis-histidinyl axial iron coordination and low redox potentials. We have purified two new cytochromes *c* with markedly different molecular masses (10 000 and 50 000) from the bacterium *Desulfuromonas acetoxidans*, which uses anaerobic sulfur respiration as its sole energy source. The characterization by electrochemistry and optical and EPR spectroscopies revealed the cytochrome *c* (M_r = 10 000) to be the first monohemic cytochrome *c* exhibiting a bis-histidinyl axial coordination and a low redox potential (−220 mV). The cytochrome *c* (M_r = 50 000) contains four hemes of low potential (−200, −210, −370, and −380 mV) with the same axial coordination. The N-terminal amino acid sequences were compared with that of the trihemic cytochrome c_7, previously described in *D. acetoxidans* and which is related to tetrahemic cytochrome c_3 from sulfate reducing bacteria. Some homology was found between cytochrome *c* (M_r = 10 000) and cytochrome c_7. Both *D. acetoxidans* cytochromes *c* are located in the periplasmic space and their biochemical and spectroscopic properties indicate that they belong to the class III cytochromes.

The microbial reduction of elemental sulfur, S^0, to hydrogen sulfide under anaerobic conditions has attracted attention during the last 100 years and has been studied by focusing on the fermentative metabolism of microorganisms (*1*). The existence of truly dissimilar sulfur-reducing bacteria was considered when a new species and genus, *Desulfuromonas acetoxidans*, was described by Pfennig and Biebl in 1976 (*1*). This organism has been classified as a strictly anaerobic Gram negative, flagellated, rod-shaped bacterium which is unable to ferment organic substances. It can grow on acetate by an anaerobic sulfur respiration as its sole energy source [acetate or ethanol can serve as carbon and energy sources and their oxidation to CO_2 is stoichiometrically linked to the reduction of elemental sulfur to sulfide (*1*,*2*)]. It was generally believed that electron transport to elemental sulfur could not yield sufficient energy for the bacterium to grow; however, in *D. acetoxidans*, the energy seems to be generated via the cytochrome-linked electron transfer systems

* Corresponding author: Tel, +33-4-91-16-41-44. Fax, +33-4-91-77-95-17. E-mail, bruschi@ibsm.cnrs-mrs.fr.
‡ Laboratoire de Bioenergetique et Ingenierie des Proteines.
§ Institut de Biologie Structurale.
|| Laboratoire d'Information Genetique et Structurale.
⊗ Abstract published in *Advance ACS Abstracts,* August 1, 1997.

S0006-2960(97)00774-5 CCC: $14.00

to either elemental sulfur or fumarate as electron acceptors and a substrate-level ATP formation involving the oxidation of ethanol to acetate (*3*).

The fact that sulfate-reducing bacteria do not use elemental sulfur (*4*) and that *Desulfuromonas* cannot use the oxidized sulfur compounds, which are electron acceptors for the sulfate-reducing bacteria, demonstrates that the reduction of these various sulfur compounds cannot be carried out the same way. It is worth mentioning that evidence is now available that cytochrome c_3, a tetraheme protein present in all sulfate-reducing bacteria of the genus *Desulfovibrio*, may act *in vitro* like a sulfur oxidoreductase (*5*).

D. acetoxidans cytochrome $c_{551.5}$, which is also known as cytochrome c_7, is a small 68 amino acid monomeric cytochrome (with a M_r of about 9100) containing three hemes. These c-type hemes are covalently thioether linked to the protein with axial bis-histidine ligation. Its sequence is largely homologous to the tetraheme cytochrome c_3 from *Desulfovibrio*, apart from the fact that the heme 2 is absent from cytochrome c_7 (*6*, *7*). Like cytochrome c_3 (*8*), these heme groups are characterized by low redox potentials (−140, −210, and −240 mV) and their orientation is similar to that of three out of the four hemes of cytochrome c_3 as shown by the structure of cytochrome c_7, recently determined from NMR spectroscopic data (*9*). As the folding of the protein is homologous to that of cytochrome c_3, it is tempting to postulate that cytochrome c_7 may function like a terminal oxidase in the electron transport to elemental sulfur.

It was recently demonstrated that *D. acetoxidans* can obtain energy for its growth by combining acetate oxidation with the dissimilar reduction of Fe(III) and Mn(IV) (*10*). Similar studies have demonstrated that cytochrome c_3 can function as a terminal Fe(III) and U(VI) reductase in *Desulfovibrio vulgaris* (*11*). Because of the similarities observed between the triheme cytochrome c_7 and the tetraheme cytochrome c_3, it is quite plausible that these low redox potential proteins may have similar metal reductase activities. Further investigations into the mechanisms and the specificity of the metal reduction are required to determine whether or not this is definitely the case.

With the aim of comparing the metabolic pathways of sulfur- and sulfate-reducing bacteria and the electron carrier proteins involved, we investigated the electron carrier content of these bacteria. Ferredoxin and rubredoxin from *D. acetoxidans* have been previously characterized (*6*). Additional electron carriers, such as (Fe-S) proteins and low-spin cytochromes *c* have been detected using EPR spectroscopy in membrane and cytoplasmic fractions (*12*).

Here we report, the purification and characterization of two new low-potential cytochromes *c* isolated from *D. acetoxidans*.

MATERIALS AND METHODS

Microorganism and Culture Growth Procedure. *D. acetoxidans* strain 5071 was grown as previously described by Pfennig and Biebl (*1*). The basal salt medium used contained 0.05% ethanol (carbon and energy sources) and 0.2% DL−sodium malate (electron acceptor). Cells were grown in a 200 L fermenter (Chemap) starting with a 40 L inoculum of fresh culture. The maximal absorbancy of $A = 0.4$ at 436 nm was reached after 18−20 h of growth. Cells were harvested by centrifugation and stored at −20 °C until use.

Optical Absorption Spectra. Visible and ultraviolet absorption spectra of the proteins were determined with a Beckman DU 7500 spectrophotometer. Molar extinction coefficients at the absorption maxima were obtained from these spectra using protein concentrations based on amino acid analysis.

Isoelectric Point Measurements. Isoelectric points were determined by performing isoelectric focusing using both a Phast Gel apparatus from Pharmacia LKB Biotechnology (*13*) and a Multiphor II system from Pharmacia. Phast Gel IEF 3−9, which operates in the 3−9 pH range, and ampholine polyacrylamide gel plates from Pharmacia (pH range 3.5−9.5) were used together with a Pharmacia broad-range pI calibration kit containing proteins with various isoelectric points ranging from 3 to 10.

Molecular Mass Determination. The molecular mass of the protein was determined by performing sodium dodecyl sulfate−polyacrylamide gel electrophoresis under reducing conditions on a Pharmacia Phast System with Phast Gel 12% polyacrylamide and Phast Gel SDS buffer strips.

Mass spectra were obtained on a Perkin-Elmer Sciex API III+ triple quadrupole mass spectrometer equipped with a nebulizer-assisted electrospray source (ionspray) operating at atmospheric pressure. A 5 kV voltage was applied to the electrospray needle. The mass spectrometer was scanned from *m/z* 800 to 2200, with steps of 0.5 *m/z* unit at a declustering potential (orifice voltage) of 80 V. The dwell time was 2 ms, and the resolution was 1 mass unit. For each mass spectrum, roughly five scans were performed. Each molecular species produced a series of multiply charged protonated molecular ions. The reconstructed molecular mass profiles were determined using a deconvolution algorithm (PE/Sciex). In flow injection analyses, samples (about 100−200 pmol) were introduced by means of a Harvard 22 syringe pump at a flow rate of 5 μL/min on a Valco C6W injector equipped with a 1 L internal loop. To promote the protonation of the proteins, a solvent containing 25% methanol and 1% acetic acid in water was used.

Analysis for Iron and Heme Content. The iron content was determined by performing plasma emission spectroscopy using a Jobin Yvon model JY 38 apparatus.

The total number of heme units was determined by means of the pyridine ferrohemochromogen test. A known mass of the protein (determined by hydrolysis of an aliquot of protein solution and performing quantitative amino acid analysis) was added to an aqueous alkaline (7.5 mM NaOH/25%) pyridine solution and reduced by adding a few crystals of sodium dithionite. The heme content was determined from the pyridine ferrohemochrome spectrum, using the millimolar absorbance coefficient of 29.1 M^{-1} cm^{-1} at 550 nm of the c_3 derivative (*14*).

Electrochemical Techniques. Electrochemical measurements were performed using a three-electrode design. The auxiliary electrode was a platinum wire and the reference electrode a calomel (KCl saturated) electrode. All the potentials mentioned are with respect to the normal hydrogen electrode. We used a pyrolytic membrane graphite electrode as the working electrode, which provides a useful tool for the electrochemical study of small amounts of proteins. The pyrolytic graphite electrode was constructed from 4 mm diameter rods of PG (Le Carbone Lorraine, Paris) housed in epoxy sheaths and cut with the disk face parallel to the basal plane. Before each electrochemical scan, the PG electrode

was polished with ultrafine emery paper, washed with water, and dried. A poly-L-lysine coating was achieved by depositing an aliquot of an 0.5% wt aqueous poly-L-lysine solution on the PG surface. The film was then left to dry in air at room temperature.

The design of the membrane graphite electrode has been previously described (*15*). Briefly, a small amount of protein solution (2 μL) was deposited onto the working PG electrode and covered with a piece of dialysis membrane (Visking PM 3000). A rubber ring was then fitted around the membrane graphite electrode body so that the entrapped protein solution formed a uniform thin layer. The membrane graphite electrode was then placed in the cell containing the supporting electrolyte.

An EGG362 scanning potentiostat was used for cyclic voltammetry. The solutions were deoxygenated by bubbling them with high-purity Argon. Measurements were performed in 100 mM Tris-HCl buffer at pH 7.6, which served as the supporting electrolyte. All experiments were carried out at 20 °C.

Poly-L-lysinehydrobromide (molecular mass > 300 000 Da) was obtained from Sigma.

Redox Titrations and EPR Spectroscopy. The spectrophotometric redox titrations were monitored by performing absorbance measurements at 553 nm with a Kontron 932 spectrophotometer on 5 μM cytochrome solution in Tris-HCl 0.1 M (pH 7.6) kept under argon atmosphere. The potentials were checked at 21 °C with a combined micro platinum Metrohm electrode and adjusted with small amounts of a concentrated solution of sodium dithionite (10 mM) in the presence of methylene blue (11 mV), 2-hydroxy 1,4-naphtoquinone (−145 mV), phenosafranine (−255 mV), benzyl viologen (−350 mV), and methyl viologen (−440 mV) at 0.6 μM concentration each.

EPR spectra were recorded on a Bruker ESP 300E spectrometer. The samples were cooled using an Oxford Instrument ESR 900 cryostat with a ITC4 temperature controller. For spin quantitations, the second integral value of the spectrum was compared to that given by a $CuSO_4$ standard recorded at the same temperature.

Amino Acid analysis and Protein Sequencing. For the amino acid analysis, protein samples were hydrolyzed in 200 μL of 6 M HCl at 110 °C for 18, 24, and 72 h, in sealed evacuated tubes, and analyzed with a Beckman amino acid analyzer (System 6300). The hemes were removed using Ambler's method (*16*), and the resulting apoprotein was isolated by gel filtration on Sephadex G25 in 5% (by vol) formic acid. Sequence determinations were carried out with an Applied Biosystems A470 gas-phase sequencer. Quantitative determination of phenylthiohydantoin derivatives was performed using high-pressure liquid chromatographic procedures (Waters Associates, Inc.), monitored with a data and chromatography control station (Waters 840).

S-carboxymethylated protein was prepared by dissolving the apoprotein in 0.5 M Tris-HCl, pH 9.0, 8 M urea, and 20 mM EDTA and performing an iodoacetic acid treatment, as described by Crestfield *et al*. (*17*).

RESULTS

Purification of the D. acetoxidans Cytochromes. All purification procedures were performed at +4 °C, and all buffers were at pH 7.6, except for the potassium phosphate buffer (pH 7.0). The cell-free extract was prepared from 280 g (wet weight) cells in 10 mM Tris-HCl buffer containing 2 mM of phenylmethanesulfonyl fluoride. The cells were subsequently broken using a Manton-Gaulin press, and the samples were centrifuged at 35 000 rpm for 1 h to remove the membranes. In the first step, the cell-free extract (1600 mL) was run through a DEAE-cellulose column equilibrated with 10 mM Tris-HCl buffer. The unadsorbed proteins containing the cytochrome c_7 were loaded onto a Bio-Gel HTP column equilibrated with 10 mM Tris-HCl, and the fraction containing the cytochrome c_7 was eluted with 600 mM potassium phosphate buffer and purified to homogeneity after a chromatography step with a Superdex 75 column on a FPLC apparatus. The adsorbed proteins were eluted from the DEAE-cellulose with 0.5 M Tris-HCl buffer. This fraction was dialyzed against 10 mM Tris-HCl overnight. The dialyzed solution was applied to a Q-Sepharose column on a FPLC apparatus. The proteins were eluted with a gradient of 100 mM NaCl to 100 mM Tris-HCl + 700 mM NaCl, pH 7.6. The first fraction was eluted to 330 mM NaCl and the second fraction to 430 mM NaCl, yielding a cytochrome *c* which was judged to be pure when tested by SDS gel electrophoresis. Its absorbance index *C*, defined as $C = (A_{553}\text{red} - A_{570}\text{red}/A_{280}\text{ox})$, was found to be 1.01. In view of the molecular weight determined by SDS−PAGE, we refer to this cytochrome as *D. acetoxidans* cytochrome *c* ($M_r = 50\ 000$). The previously described first fraction obtained after dialysis was loaded onto a HTP column equilibrated with 10 mM Tris-HCl buffer. A red fraction was eluted. After dialysis, this fraction was run through a Superdex 75 column (FPLC apparatus). The cytochrome eluted from this column was found to be pure by SDS gel electrophoresis. Its absorbance index *C* was found to be 1.14. Given its molecular weight, this cytochrome was named *D. acetoxidans* cytochrome *c* ($M_r = 10\ 000$).

As the result of the purification procedure, three different cytochromes *c* were found to be present in *D. acetoxidans*: the trihemic cytochrome c_7 and two acidic cytochromes. Judging by the yield of purification, we obtained 30 mg of cytochrome c_7, 3 mg of cytochrome *c* ($M_r = 10\ 000$), and 20 mg of cytochrome *c* ($M_r = 50\ 000$). The isoelectric points are, respectively, 7.77 for cytochrome c_7, 6.7 for cytochrome *c* ($M_r = 10\ 000$), and 6.55 for cytochrome *c* ($M_r = 50\ 000$).

Molecular Mass. The apparent molecular mass deduced from the SDS−PAGE Analysis was about 10 000 and 50 000 with the native form and after boiling the sample for 1 min, respectively.

The mass spectra showed that the two cytochromes are monomeric cytochromes with molecular masses of 10 591.1 Da in the case of cytochrome *c* ($M_r = 10\ 000$) and 51 240.5 Da in that of cytochrome *c* ($M_r = 50\ 000$).

Optical Spectra. The ultraviolet−visible spectrum of the purified cytochrome *c* ($M_r = 10\ 000$) exhibited a Soret peak at 409 nm in the oxidized state and peaks at 419, 523, and 553 nm in the dithionite reduced form. The absorption coefficient of reduced cytochrome at 553 nm was 21 787 M^{-1} cm^{-1}, and the α/β ratio of reduced cytochrome was 1.68 and α red/α ox was 3.05. The absorption coefficient of the cytochrome *c* ($M_r = 50\ 000$) reduced state at 552 nm was 148 100 M^{-1} cm^{-1}. The α/β ratio of the reduced form was 1.76, and the ratio α red/α ox was 3.57. The optical spectra of the two cytochromes did not exhibit the charac-

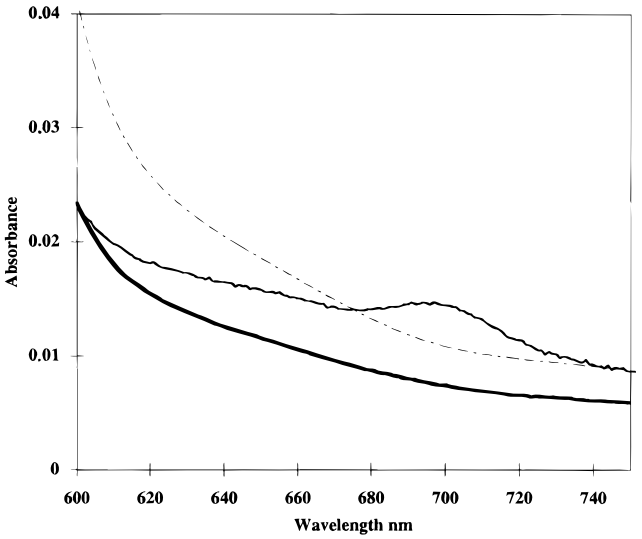

FIGURE 1: Comparative optical spectra in the 600−760 nm range of (plain line) Horse heart cytochrome *c*, 200 μM, (bold line) *Desulfuromonas acetoxidans* cytochrome *c* (M_r = 10 000), 200 μM, and (dashed line) *D. acetoxidans* cytochrome *c* (M_r = 50 000), 400 μM (absorbance has been divided by a factor 2). Tris-HCl buffer, 0.1 N, pH 7.6. Path length = 0.5 mm.

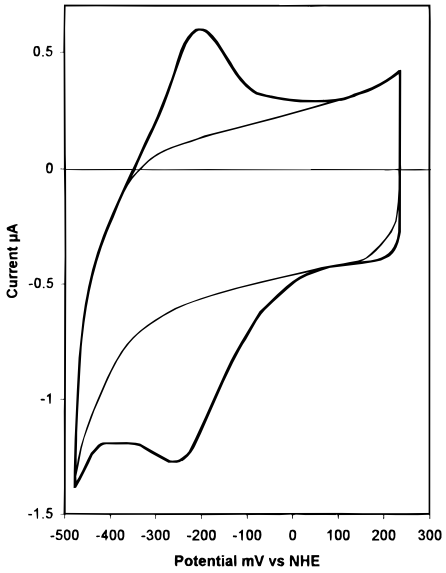

FIGURE 2: Cyclic voltammetry of *D. acetoxidans* cytochrome *c* (M_r = 10 000) in a thin layer configuration at the membrane graphite electrode-poly-L-lysine modified electrode prepared by depositing 0.5 μL of poly-L-lysine on the pyrolytic graphite electrode, 0.1 M Tris-HCl buffer, pH 7.6, −20 mV/s, without (plain line) and with (bold line) cytochrome *c* (M_r = 10 000) added.

teristic 695 nm band (Figure 1) thought to reflect the environment and the strength of the heme iron−methionine sulfur bond.

Iron and Heme Determination. The iron content as determined by performing plasma emission spectroscopy was 1 atom of iron/molecule with cytochrome *c* (M_r = 10 000) and 4 atoms of iron/molecule with cytochrome *c* (M_r = 50 000).

The number of heme groups per molecule was calculated and found to be 1 and 4, respectively, with cytochrome *c* (M_r = 10 000) and cytochrome *c* (M_r = 50 000), using the millimolar absorbance coefficient of 29.1 at the peak of the pyridine ferrohemochrome of the two cytochromes.

Electrochemical Characterization. It has been reported that the membrane electrode enables the direct electrochemistry (*15*). In this work, this electrode was first tested to determine the electrochemical behavior of the low redox potential cytochrome c_7. One electrochemical wave with a marked shoulder at more positive potentials was recorded, in line with the classical laws of thin layer electrochemistry. Deconvolution in three electrochemical processes yielded three midpoint potentials of −140, −200, and −220 mV, respectively, which is in good agreement with previous results (*18*). However poor electrochemical signals were obtained when studying cytochrome *c* (M_r = 10 000) and cytochrome *c* (M_r = 50 000) with a bare membrane electrode. An improvement of the charge transfer was obtained by applying a poly-L-lysine coating to the graphite surface. It has been clearly established that electrostatic interactions between the electrode surface and the overall negative charge of proteins at pH 7.6 improves the electrochemical response obtained at the modified electrode (*19*). A typical cyclic voltammogram obtained at the modified poly-L-lysine membrane electrode is shown in Figure 2, for a 200 M solution of cytochrome *c* (M_r = 10 000) entrapped between the membrane and the graphite surface. The electrochemical signal was characterized by a single well-defined wave at a midpoint potential of E_m = −230 mV. This makes this protein very interesting, since it is the first monohemic cytochrome exhibiting such a low redox potential. The cathodic peak current varied linearly with increasing sweep rates as was to be expected when working in a thin layer configuration. The peak to peak separation decreased with decreasing sweep rates but was still 30 mV at 5 mV/s, which indicated that we are dealing with a quasi-reversible electrochemical process. In the range 3 < pH < 12, no pH dependence was observed on the redox potential E_m. On the other hand, the E_m increased slightly when the amount of poly-L-lysine deposited on the electrode increased, again reflecting the occurrence of electrostatic interactions between cytochrome *c* (M_r = 10 000) and the positively charged poly-L-lysine membrane modified graphite electrode.

The direct electrochemistry of cytochrome *c* (M_r = 50 000) was expected to be much more complex. Up to date, only a few electrochemical studies have been performed on proteins with molecular mass greater than 30 000 Da. Actually irreversible denaturation of high molecular mass proteins often occurs at the electrode. The electrochemical data on cytochrome *c* (M_r = 50 000) seem to indicate that a decoordination of the axial histidine had occurred. Indeed the electrochemical signal produced by cytochrome *c* (M_r = 50 000) at the poly-L-lysine modified membrane electrode was characterized by a cathodic peak at −260 mV and an anodic peak at −90 mV on the reverse scan. This large peak to peak separation indicates a reversible rearrangement of the reduced cytochrome. As a positive shift in the redox potentials was recorded both at more acidic pH levels, at which the histidine may have been protonated, and when the protein was directly adsorbed at the graphite electrode, this rearrangement presumably has to do with axial histidine decoordination.

Spectrophotometric Titration. With both cytochromes, the redox behavior was monitored by studying the variation of band (553 nm) as a function of the solution potential.

With cytochrome *c* (M_r = 10 000), the experimental data fitted a Nernstian curve centered at −220 ± 10 mV (Figure 3), in good agreement with electrochemical measurements.

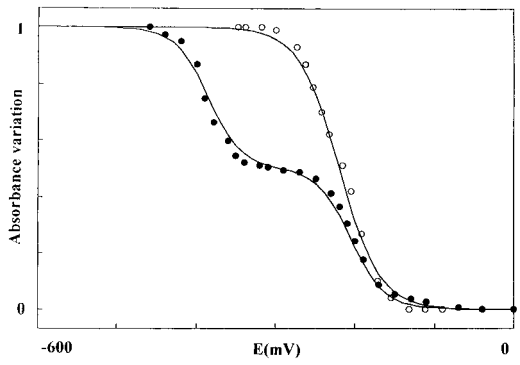

FIGURE 3: Reductive titration of *D. acetoxidans* cytochromes with dithionite monitored by performing optical absorbance measurements at 553 nm. The normalized variations correspond to the ratio $(A_{553(E)} - A_{553(ox)})/(A_{553(rd)} - A_{553(ox)})$. Solid lines give the best fit between the data and the Nernst curves: open circles, cytochrome *c* ($M_r = 10\,000$): Nernst curve centered at −220 mV; filled circles, cytochrome *c* ($M_r = 50\,000$). Four Nernst curves of equal amplitude centered at −200, −210, −370, and −380 mV.

With cytochrome *c* ($M_r = 50\,000$), two distinct redox type centers (∼−200 mV and ∼−370 mV) appeared to be involved in the electron transfer. The continuous curve reported in Figure 3 is the one giving the best fit upon adding the contribution of four Nernstian curves of the same amplitude centered at −200, −210, −370, and −380 mV, respectively.

EPR Spectroscopy. The EPR spectra of both oxidized cytochromes from *D. acetoxidans* were recorded at 15 K. The cytochrome *c* ($M_r = 10\,000$) gave a rhombic spectrum typical of a low-spin heme protein with **g** values at 2.91, 2.27, and 1.56 (Figure 5a). Its signal intensity corresponded to 1 ± 0.2 spin/molecule.

The cytochrome *c* ($M_r = 50\,000$) exhibited a more complex EPR spectrum with features at $\mathbf{g} = 3.02, 2.93, 2.65, 2.26, 1.58$, and 1.36. A broad line with a weaker amplitude was also visible at about $\mathbf{g} = 3.4$. The double integration of the whole spectrum gave an intensity of 3.9 ± 0.3 spins/molecule, which confirms the presence of four heme groups in the protein. In all tetrahemic cytochromes, the three-dimensional structure of which has been determined, the four hemes are axially coordinated by two histidine residues. In this scheme of coordination, the g-tensors of the hemes depend strongly on the relative orientation of the axial ligands, since the **g**-tensor anisotropy increases with the angle between the normal to imidazole planes (*20*−*22*). The positive peaks observed at $\mathbf{g} > 2.8$ are likely associated with the components at $\mathbf{g} = 2.26$ and 1.36 and are consistent with the presence of heme groups with a bis-histidinyl coordination, but the origin of the lines around $\mathbf{g} = 2.65$ is less clear. According to the t_{2g} hole model which accounts for the magneto-structural relationships in the case of low-spin hemoproteins (*23*, *24*), a $\mathbf{g}_z$ value close to 2.6 will be associated with spectral components at about $\mathbf{g}_Y = 2.4$ and $\mathbf{g}_X = 1.7$. No particular spectral feature is visible at these **g** values, suggesting that the $\mathbf{g} = 2.65$ peaks are not $\mathbf{g}_Z$ type lines of heme groups. Another striking feature of the spectrum is the derivative-like peak centered at $\mathbf{g} = 1.58$ (Figure 5b). This line was present with the same relative amplitude in all the cytochrome *c* ($M_r = 50\,000$) preparations, which rules out the possibility that it may be due to an adventitious paramagnetic species. According to the t_{2g} model, a $\mathbf{g}_Y$ line centered at $\mathbf{g} = 1.58$ is characteristic of a highly anisotropic **g** tensor with $\mathbf{g}_z > 3.5$ (*23*, *24*), as is known to occur in the case of the b-type hemes present in the membrane-bound electron transfer complexes of mitochondria and chloroplasts. However, this explanation for the $\mathbf{g} = 1.58$ line is not very plausible, since with the b-type cytochromes only the positive peak at $\mathbf{g}_z > 3.5$ is usually visible, while the other features are too broad to be detected (*20*). An alternative explanation is that the features at $\mathbf{g} = 2.65$ and 1.58 may be additional lines resulting from magnetic interactions between heme groups. This hypothesis was confirmed using the simulation program POINTDIP we developed to analyze the spin−spin coupling between two paramagnetic species with spins $S = {}^1/_2$ (*26*,*27*). Numerical calculations showed that the $\mathbf{g} = 2.65$ and 1.58 lines cannot be accounted for in terms of only the magnetic dipolar interactions between heme groups, even in the case of the shortest Fe−Fe distance (11 Å) ever observed in tetraheme cytochromes (*28*). Actually, these lines are reminiscent of the additional features generated by intercenter exchange interactions (*29*). Satisfactory simulations of these lines were obtained upon taking two hemes with **g** values at 2.93, 2.26, and 1.36 magnetically coupled by an exchange interaction of about 25×10^{-3} cm^{-1}, the *z* axes of the two hemes being nearly parallel.

Amino acid Analysis and N-terminal Sequence Determination. The amino acid composition of cytochrome *c* ($M_r = 10\,000$) was determined by performing amino acid analysis on the basis of the molecular mass of the protein (10 591 Da). This analysis showed the presence of three cysteine residues, which is in agreement with the presence of one heme per molecule (Table 1). The isoelectric point of this cytochrome has been found to be 6.7, which is in agreement with its low lysine and arginine residue contents.

The amino acid composition of cytochrome *c* ($M_r = 50\,000$) is in good agreement with the molecular mass of 51 240 Da measured using mass spectrometric methods. It contains 12 cysteine, 14 histidine, and six tryptophane residues for a total number of 443 amino acids. Its isoelectric point has been measured and found to be 6.55.

The N-terminal sequence determination of cytochrome *c* ($M_r = 10\,000$) up to the 33nd residue shows some homologies with the amino acid sequence of cytochrome c_7, especially in the heme binding site position which is homologous with the heme 1 of cytochrome c_7 position (Figure 4). The His residue, the sixth axial ligand of heme 1, is in the same position (residue 17 in cytochrome c_7 numbering) but the His in position 20, which is linked to heme 3 in cytochrome c_7 and cytochromes c_3 from sulfate reducing bacteria, is replaced by a Phe residue.

The N-terminal sequence of cytochrome *c* ($M_r = 50\,000$) up to the 30nd residue does not show any homologies with the amino acid sequences of cytochromes c_3 or cytochrome c_7 and does not contain a heme binding site.

DISCUSSION

Multihemic cytochromes described to date in sulfate- and sulfur-reducing bacteria exhibit no structural similarities with the other cytochrome *c* classes and are associated with the divergent respiratory modes involving the use of elemental sulfur or oxidized sulfur compounds as terminal acceptors. Ambler (*30*) has classified the multihemic proteins including triheme, tetraheme, and octaheme proteins characterized by

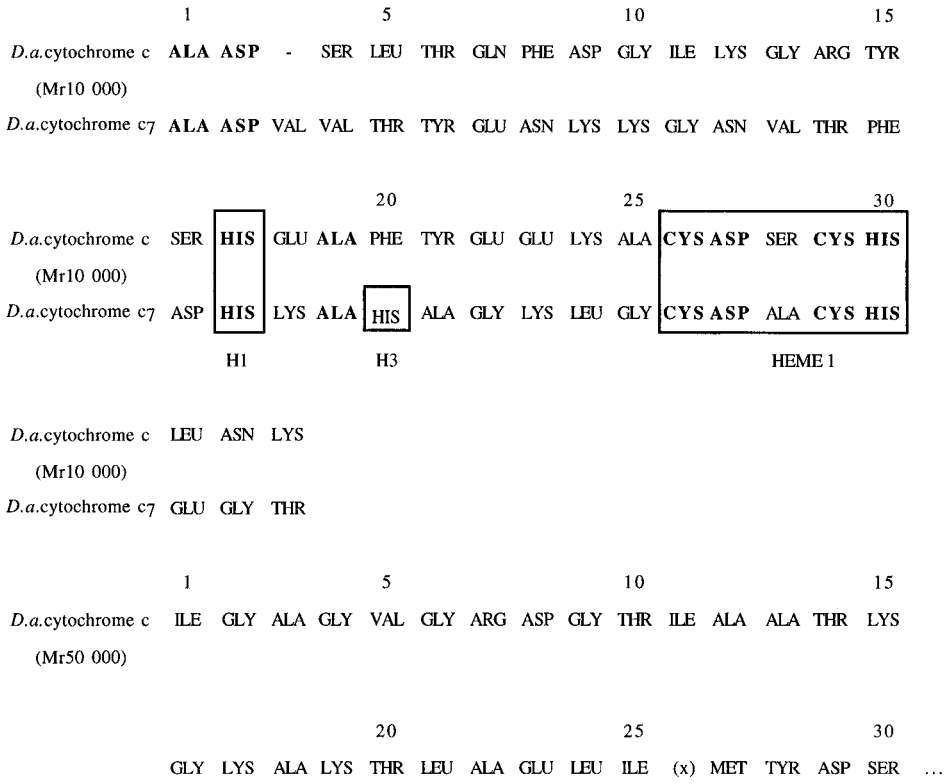

FIGURE 4: N-terminal sequences of *D. acetoxidans* cytochrome c_7, cytochrome *c* (M_r = 10 000), and cytochrome *c* (M_r = 50 000). The heme attachment sites have been boxed and numbered as they occur in the sequence. The sixth histidine axial ligand is indicated for the cytochrome c_7 hemes. The numbers above the histidines residues correspond to the heme binding site with which they are associated, according to the three dimensional structure determination of cytochrome c_7 (*9*). Residues common to several proteins are highlighted. X corresponds to an unidentified amino acid.

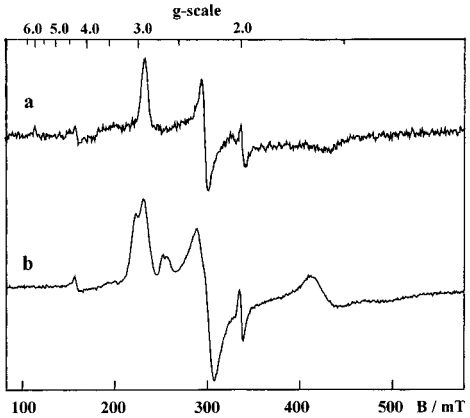

FIGURE 5: EPR spectra given by cytochromes *c* from *D. acetoxidans* (a) oxidized cytochrome *c* (M_r = 10 000) and (b) oxidized cytochrome *c* (M_r = 50 000). Experimental conditions: temperature, 15 K; microwave frequency, 9.416 GHz; microwave power, 1 mW; and modulation amplitude, 1 mT.

a bis-histidinyl iron coordination, as belonging to class III of the c-type cytochromes. On the basis of (1) the amino acid sequence of a high molecular mass cytochrome *c* (M_r = 65 600) containing 16 hemes (*31*), (2) the X-ray crystallographic comparisons between the tetraheme cytochrome c_3 (M_r = 13 000) (*32*), and (3) the octaheme cytochrome c_3 (M_r = 26 000) (*28*), we have proposed that all these cytochromes belong to the cytochrome c_3 superfamily and that they have a common ancestral origin (*33*).

In this study, we have characterized a cytochrome *c* (M_r = 10 000), which has the same characteristics as the other members of the class III cytochromes, namely a bis-histidinyl coordination and a low redox potential, that is the first monohemic cytochrome found, so far, to exhibit these characteristics. Upon aligning its N-terminal sequence with that of cytochrome c_7, some homology was observed between the heme binding site and between the position of the His, sixth axial ligand (Figure 4), indicating an evolutionary relationship between the two cytochromes.

In the case of the multihemic cytochromes with a high molecular mass, a hexaheme protein, which has nitrite reductase activity (*34*), hexadecaheme cytochromes from *D. vulgaris* Hildenborough, Miyazaki (*35*), and *D. gigas* (*36*), and more recently a dodecaheme cytochrome *c* from *D. desulfuricans* with a molecular mass of 37 768 Da characterized by the bis-histidinyl coordination (*37*), have been described. In all of these cytochromes, the presence of more than four hemes is correlated with a greater molecular mass than that of the tetrahemic cytochrome c_3 (M_r = 13 000). In the case of *D. acetoxidans* cytochrome *c* (M_r = 50 000), the four hemes are linked to a larger polypeptide chain. The number of cysteine and histidine residues is compatible with the presence of four hemes which is confirmed by EPR spectroscopy. The **g** values of the four heme groups are consistent with a bis-histidinyl axial coordination but only the absence of significant visible absorption at 695 nm enable us to rule out His−Met residues at the fifth and sixth coordination positions which characterize cytochromes *c* of class I. Interestingly, the magnetic interactions observed between at least two heme groups of the cytochrome *c* (M_r = 50 000) are an unusual feature of tetrahemic cytochromes. In all known three-dimensional structure of cytochromes c_3, the compact arrangement of the hemes leads to iron to iron distances ranging from 11 to 18 Å (*28*). We have shown that for such distances, the spectral effects of magnetic

Table 1: Amino Acid Compositions of *D. acetoxidans* Cytochrome *c* (M_r = 10 000) and (M_r = 50 000)[a]

	cytochrome *c* (M_r = 10 000) amino acid mol residues (mol)	cytochrome *c* (M_r = 50 000) amino acid mol residues (mol)	cytochrome c_7
aspartic acid	10.8 (11)	39.5 (39)	9
threonine[b]	3.9 (4)	34.9 (35)	5
serine[b]	5.9 (6)	23.5 (24)	2
glutamic acid	14.0 (14)	53.4 (53)	3
proline	3.9 (4)	21.7 (22)	2
glycine	6.1 (6)	40.9 (41)	6
alanine	7.2 (7)	35.2 (35)	8
cysteine[c]	(3)	12.0 (12)	6
valine	5.8 (6)	21.6 (22)	3
methionine	1.9 (2)	15.8 (16)	0
isoleucine	3.7 (4)	21.7 (22)	3
leucine	6.0 (6)	28.6 (29)	1
tyrosine	1.9 (2)	14.9 (15)	1
phenylalanine	2.8 (3)	13.4 (14)	1
histidine	2.8 (3)	14.3 (14)	6
lysine	4.7 (5)	25.1 (25)	12
arginine	2.7 (3)	19.0 (19)	0
tryptophane[d]	0 (0)	6.0 (06)	0
total number of residues	89	443	68

[a] The results were obtained by analyzing 24, 48, and 72 h hydrolysates. Comparisons were made with the amino acid composition of *D. acetoxidans* cytochrome c_7 based on the amino acid sequence of the latter (*7*). [b] The values given for threonine and serine were extrapolated from the hydrolysis times. [c] Analyzed as carboxymethylcysteine. [d] Analyzed according to Peuke *et al.* (*43*).

dipolar interactions are hidden by the line widths of heme signals and cannot be detected by EPR spectroscopy (*29*). In cytochrome *c* (M_r = 50 000) the EPR detectable spin−spin coupling arises from a strong exchange interaction between two hemes and is likely to be due to a peculiar protein medium between these hemes. This could be related to the high tryptophane content of this cytochrome which favors the overlap of the magnetic orbitals of heme groups. The redox potentials measured in the case of cytochrome c_7 (−140, −210, and −240 mV), cytochrome *c* (M_r = 10 000) (−220 mV), and cytochrome *c* (M_r = 50 000) (−200, −210, −370, and −380 mV) are on the same range of that of the cytochromes c_3. These low redox potentials are also in agreement with the idea that these cytochromes, like cytochrome c_3 (M_r = 13 000), should be classified in class III. It is worth noting that the bis-histidinyl coordination is associated with a negative redox potential. The effects of this type of coordination have been quantified using a site-directed mutagenesis approach. The four variant molecules, each carrying a single His−Met replacement, show an increase in the redox potential of the corresponding heme group of at least +150 mV (*38*).

The genes of *D. vulgaris* Hildenborough cytochrome c_{553}, cytochromes c_3 (M_r = 13 000), and cytochromes Hmc have been cloned, and their sequences show the presence of a cleavable NH_2 terminal signal peptide directing the export of the apopolypeptide to the periplasm (*39*). The N-terminal sequences of *D. acetoxidans* cytochromes c_7 and *c* (M_r = 10 000) are compatible with the presence of a signal peptidase cleavage site (Ala−Asp) as defined by Le Gall *et al.* (*40*). However, the N-terminal sequence Ile−Gly of the cytochrome *c* (M_r = 50 000) was not described by these authors as a signal peptidase site. It should be noted that, although the (Glu−Thr) sequence of *D. desulfuricans* Norway cytochrome c_3 (M_r = 26 000) and the (Lys−Ala) sequence of *D. vulgaris* Hmc have not been described as N-terminal signal peptidase, upon the cloning of both genes, the presence of a signal peptide and the periplasmic location of these cytochromes were established (*41*). In addition, all these cytochromes have been recovered with a high yield after isolating from the periplasmic proteins using the method described by Westen *et al.* (*42*), whereby the cells were suspended in 50 mM Tris-HCl and 50 mM EDTA at pH 9.0 and stirred for 15−20 min at 37 °C. In the case of *D. acetoxidans*, we performed the cytochromes c_7, cytochrome *c* (M_r = 10 000), and cytochrome *c* (M_r = 50 000) purification using this method, which yielded the same amount of each cytochrome as when the cells had been treated through a Manton−Gaulin press. This suggests that these cytochromes, like the *Desulfovibrio* cytochromes, may have a periplasmic location.

The exact functional roles of the three cytochromes from *D. acetoxidans* characterized in the present study have not yet been established. Further studies that will include physiological tests, genetic investigations, and comparisons between the three-dimensional structures of the various cytochromes are required in order to establish their specificity toward their redox partners.

ACKNOWLEDGMENT

We gratefully acknowledge the contribution of the Fermentation Plant Unit (L. C. B., Marseille, France) for growing the bacteria and of N. Zylber and J. Bonicel (Protein Sequencing Unit, B. I. P., Marseille, France) for performing the amino acid analysis and N-terminal sequence determination. We also thank Dr. Jean-Claude Germanique for the iron content analysis and Dr. David Robertson for his critical reading of the manuscript.

REFERENCES

1. Pfennig, N., and Biebl, H. (1976) *Arch. Microbiol. 110*, 115−117.
2. Pfennig, N., and Biebl, H. (1981) in *The prokaryotes. A handbook on habitats, isolation and identification of bacteria* (Starr, M. P., Stolp, H., Trüper, H. G., Belows, and A. Schegel, H. G., Eds.) pp 941−947, Springer, Berlin, Heidelberg, New York.
3. Barker, H. A. (1972) in *Horizons of bioenergetics* (San Pietro, A., Gest, H., Eds.) pp 7−31, Academic Press, New York.
4. Postgate, J. R. (1951) *J. Gen. Microbiol.* 5, 725−738.

5. Fauque, G., Hervé, D., and Le Gall, J. (1979) *Arch. Microbiol. 121*, 261−264.
6. Probst, I., Bruschi, M., Pfennig, N., and Le Gall, J. (1977) *Biochim. Biophys. Acta 460*, 58−64.
7. Ambler, R. P. (1971) *FEBS Lett.* 351−353.
8. Bruschi, M., Loutfi, M., Bianco, P., and Haladjian, J. (1984) *Biochem. Biophys. Res. Commun. 120*, 384−389.
9. Banci, L., Bertini, I., Bruschi, M., Sompornpisut, P., and Turano, P. (1996) *Proc. Natl. Acad. Sci. U.S.A. 93*, 14396−14400.
10. Roden, E. E., and Lovley, D. R. (1993) *Appl. Environ. Microbiol. 59*, 734−742.
11. Lovley, D. R., Widman, P. K., Woodwark, J. C., and Philipps, E. J. P. (1993) *Appl. Environ. Microbiol. 59*, 3572−3576.
12. Bache R., Kroneck P. M. H., Merkle H., and Beinert H. (1983) *Biochim. Biophys. Acta* 417−426.
13. Haff, L. A., Fagerstam, L. A., and Barry, A. R. (1983) *J. Chromatogr. 266*, 409−425.
14. Falk, J. E. (1964) *Porphyrins and Metalloporphyrins; Their General Physical and Coordination Chemistry and Laboratory Methods*, p 240, Elsevier, New York.
15. Haladjian, J., Bianco, P., Nunzi, F., and Bruschi, M. (1994) *Anal. Chem. Acta 289*, 15−20.
16. Ambler, R. P. (1963) *Biochem. J. 89*, 349−378.
17. Crestfield, A. M., Moore, S., and Stein, W. H. (1963) *J. Biol. Chem. 238*, 622−627.
18. Bianco, P., and Haladjian, J. (1981) *Bioelectrochem. Bioenerg. 8*, 239−245.
19. Haladjian, J., Bianco, P., Bruschi, J., and Nunzi, F. (1994) *Anal. Chim. Acta* 289, 15−20.
20. Salerno, J. C. (1984) *J. Biol. Chem.* 259, 2331−2336.
21. Walker, A., Huynh, B. H., Sheidt, W. R., and Osvath, S. R. (1986) *J. Am. Chem. Soc. 108*, 5288−5297.
22. Hatano, K., Safo, M. K., Walker, A., and Scheidt, W. R. (1991) *Inorg. Chem. 30*, 1643−1650.
23. Bohan, T. L. J. (1977) *J. Magn. Reson. 26*, 109−118.
24. More, C., Gayda, J. P., and Bertrand, P. (1990) *J. Magn. Reson. 90*, 486−499.
25. Bertrand, P., Asso, M., Mbarki, O., Camensuli, P., More, C., and Guigliarelli, B. (1994) *Biochimie 76*, 546−536.
26. Guigliarelli, B., Guillaussier, J., More, C., Setif, P., Bottin, H., and Bertrand, P. (1993) *J. Biol. Chem. 261*, 900−908.
27. Guigliarelli, B., More, C., Fournel, A., Asso, M., Hatchikian, E. C., Williams, R., Cammack, R., and Bertrand, P. (1995) *Biochemistry 34*, 4781−4790.
28. Czjzek, M., Payan, F., and Haser, R. (1994) *Biochimie 76*, 546−553.
29. More, C., Camensuli, P., Dole, F., Guigliarelli, B., Asso, M., Fournel, A., and Bertrand, P. (1996) *J. Bioinorg. Chem. 1*, 152−161.
30. Ambler, R. P. (1980) in *From cyclotrons to cytochromes* (Robinson, A. B., and Kaplan, N. O., Eds.) pp 263, Academic Press, London.
31. Pollock, W. B. R., Loutfi, M., Bruschi, M., Rapp-Giles, B. J., Wall, J. D., and Woordouw, G. (1991) *J. Bacteriol. 173*, 220−228.
32. Czjzek, M., Guerlesquin, F., Bruschi, M., and Haser, R. (1996) *Structure 4*, 395−404.
33. Bruschi, M. (1994) *Methods Enzymol. 243*, 140−155.
34. Liu, M. C., Costa, C., and Moura, I. (1994) *Methods Enzymol. 243*, 303−319.
35. Higuchi, Y., Yagi, T., and Voordouw, G. (1994) *Methods Enzymol. 243*, 155−165.
36. Chen, L., Pereira, M. M., Teixeira, M., Xavier, A. V., and Le Gall, J. (1994) *FEBS Lett. 347*, 295−299.
37. Coelho, A. V., Matias, P. M., Sieker, L. C., Moras, J., Corrondo, M. A., Lampreia, J., Costa, C., Moura, J. J. G., Moura, I., and Le Gall, J. (1996) *Acta Crystallogr. D 52*, 1202−1209.
38. Dolla, A., Florens, L., Bianco, P., Haladjian, J.,Voordouw, G., Forest, E., Guerlesquin, F., and Bruschi, M. (1994) *J. Biol. Chem. 269*, 6340−6346.
39. Pollock, W. B. R., and Woordouw, G. (1994) *Biochimie 76*, 554−560.
40. Le Gall, J., and Peck, H. D., Jr. (1987) *FEMS Microbiol. Rev. 46*, 35−40.
41. Aubert, C., Leroy, G., Bruschi, M., Wall, J. D., and Dolla, A. (1997) *J. Biol. Chem. 272*, 15128−15134.
42. Van der Westen, H. M., Mayhew, S. G., and Veeger, C. (1978) *FEBS Lett. 86*, 122−126.
43. Peuke, B., Ferenczi, R., and Kovacs, K. (1974) *Anal. Biochem. 60*, 45−50.

BI9707741